Scale space searches for a periodic signal in fMRI data with spatially varying hemodynamic response

K.J. Worsley[1], M. Wolforth[2] and A.C. Evans[2]

January 2, 1997

[1]*Department of Mathematics and Statistics, McGill University, 805 Sherbrooke St. West, Montreal, Québec, Canada H3A 2K6, and* [2]*McConnell Brain Imaging Centre, Montreal Neurological Institute, 3801 University Street, Montreal, Québec, Canada H3A 2B4*

We propose a simple method for testing for a periodic signal in fMRI data where the hemodynamic response function is spatially varying with possibly different lags at different voxels. At each voxel, the test is based on the power of the spectrum at a frequency that matches the signal, divided by an estimator of the variance to produce a χ^2 image with 2 degrees of freedom. We then apply scale space methods to search for signals of different width by smoothing the data with different Gaussian spatial filters, then searching over scale as well as location. The resulting scale space image is thresholded at a level chosen to control the false positive rate using a new result for the P-value of the maximum of scale space χ^2 fields.

Running title: Scale space searches of fMRI Data

Addresses of corresponding author:
e-mail: worsley@math.mcgill.ca
web: http://www.math.mcgill.ca/∼keith
ph: 1-514-398-3842
fax: 1-514-398-3899.

1 Introduction

In a simple fMRI experiment, the subject is presented with a periodic stimulus $x(t)$ at time t and the blood flow response $Y(\mathbf{s}, t)$ is measured at a spatial location $\mathbf{s}$ (in D dimensions) and time t. Friston *et al.* (1994a, 1995) have modeled the noise component of $Y(\mathbf{s}, t)$ as a stationary Gaussian process in both space and time. The signal component of $Y(\mathbf{s}, t)$ at a fixed location is modeled as the convolution of $x(t)$ with a hemodynamic response function, itself modeled as a Gaussian function with a lag of 8 seconds and a standard deviation of $\sqrt{8}$ seconds. The signal is then detected by cross-correlating $Y(\mathbf{s}, t)$ with $x(t)$ filtered by the hemodynamic response function, divided by an estimate of the standard deviation, to produce a Gaussian random field $Z(\mathbf{s})$ (Worsley & Friston, 1995). $Z(\mathbf{s})$ is then searched for local maxima and the P-value is assessed using standard methods based on the size of the search region and the spatial smoothness of the data (Friston *et al.*, 1994b; Worsley *et al.*, 1996a).

Some authors (Bullmore *et al.*, 1996; Lange & Zeger, 1996) have suggested that the hemodynamic response differs from location to location and in particular that the lag is spatially varying. This suggests convolving the data with a spatially varying hemodynamic response, but since the nature of the spatial variability is unknown this is not possible. An alternative, suggested by Bullmore *et al.* (1996), is to cross-correlate the data with $\sin(2\pi t/T)$ and $\cos(2\pi t/T)$, where T is the period of the stimulus, to produce two Gaussian images $Z_1(\mathbf{s})$ and $Z_2(\mathbf{s})$ (after division by an appropriate estimate of the standard deviation), then taking the sum of squares $U(\mathbf{s}) = Z_1(\mathbf{s})^2 + Z_2(\mathbf{s})^2$. This is the (standardised) power spectrum of the temporal process at a frequency matching that of the stimulus, and it should be sensitive to any periodic signal irrespective of the hemodynamic response. The only requirement is that the hemodynamic response is a *linear* filter. It is then easy to show that the resulting image $U(\mathbf{s})$ is a χ^2 random field with 2 degrees of freedom. P-values for local maxima of such a field can be found from Worsley *et al.* (1996a).

2 Scale space

Our main interest here is to apply scale space searches to look for signals of any extent. This method, first introduced by Poline & Mazoyer (1994), smoothes the data with a Gaussian filter of varying width or scale, thus adding one extra scale dimension to the data. The scale space data is then searched for local maxima in location as well as scale. The motivation for this comes from the Matched Filter Theorem (see for example Rosenfeld & Kac, 1982) which states that a signal in a background of white noise is best detected by smoothing with a filter whose shape matches that of the signal. If the signal is Gaussian-shaped with unknown width, then this suggests smoothing with a Gaussian filter of varying width. An added benefit is that the location and scale at the scale space local maximum estimates the location of the signal *and* its scale. This method was successfully applied to PET data by Worsley *et al.* (1996b) to detect signals varying from 6mm FWHM to 22mm FWHM that were missed at an intermediate filter width.

The key to the success of this method is setting a threshold for the scale space local maxima that controls the false positive rate. Assessing the significance of the local maxima,

taking into account the search over scale as well as location, was solved for Gaussian data by Siegmund & Worsley (1995) and applied to PET data in Worsley *et al.* (1996b).

3 χ^2 fields

The purpose of this paper is to extend scale space ideas to χ^2 fields, defined as the sum of squares of standard Gaussian images each with zero mean and unit variance. The motivation for this is as follows. Suppose we have $\nu \geq 1$ independent Gaussian images or SPMs, each of which contains signal at the same location and scale, but at different amplitudes. Such data could arise from an experiment where several different types of signal are expected to produce activation at the same location and scale, but with different strengths, such as a set of pain stimuli or linguistic tasks. We wish to combine information from each image in order to make an overall test of any activation. A natural test statistic is the sum of squares of the Gaussian images, which is a χ^2 field with ν degrees of freedom. If the scale is also unknown, the Gaussian images should be smoothed with the same filter, to produce scale space Gaussian images, and then the sum of squares defines the scale space χ^2 image. Note that the component Gaussian images are smoothed, not the χ^2 image itself. It can be shown that this gives the maximum likelihood estimate of the location and scale of the signal (see Worsley, 1997).

Formally, suppose that the component Gaussian fields are modeled as

$$Z_i(\mathbf{s}) = \beta_i f[(\mathbf{s} - \mathbf{s}_0)/w_0] + W(\mathbf{s}), \quad i = 1, \ldots, \nu,$$

where β_i is an unknown amplitude, f is the functional shape of the signal, $\mathbf{s}_0$ is an unknown location, w_0 is an unknown scale, and W is standard Gaussian white-noise (uncorrelated) error. In other words, the unknown location and scale of the signal are common to each component, but the amplitudes are different. We wish to test the null hypothesis of no signal, that is

$$H_0 \ : \ \beta_i = 0, \quad i = 1, \ldots, \nu.$$

To do this, each component is then smoothed by a filter with the same shape as the signal and width w, to produce scale space Gaussian images:

$$Z_i(\mathbf{s}, w) = K w^{-D/2} \int f[(\mathbf{h} - \mathbf{s})/w] Z_i(\mathbf{h}) d\mathbf{h}, \quad i = 1, \ldots, \nu,$$

where D is the number of dimensions (components of $\mathbf{s}$) and the scaling constant K is chosen so that the variance remains at one, that is

$$K = \left(\int f[\mathbf{h}]^2 d\mathbf{h} \right)^{-1/2},$$

(see Worsley *et al.*, 1996b). Then the scale space χ^2 image is defined as

$$U(\mathbf{s}, w) = \sum_{i=1}^{\nu} Z_i(\mathbf{s}, w)^2.$$

The hypothesis of no signal is rejected for large values of

$$U_{\max} = \max_{\mathbf{s},w} U(\mathbf{s}, w),$$

where the maximum is taken over all locations $\mathbf{s}$ in a search region and all widths in an interval from w_1 to w_2.

In practice, a convenient choice of smoothing filter is the Gaussian filter with unit FWHM:

$$f[\mathbf{h}] = \exp[-(4\log_e 2)\mathbf{h}'\mathbf{h}],$$

for which $K = [8(\log_e 2)/\pi]^{D/4}$. With this choice of filter, w is the FWHM.

4 P-value of the maximum

Worsley (1997) derives an approximate formula for the P-value of the maximum of a D-dimensional scale space χ^2 image searched over a range of Gaussian filter widths from w_1 to w_2 FWHM. The result, which is accurate for search regions of almost all shapes and sizes, is:

$$\mathrm{P}(U_{\max} \geq u) \approx \sum_{d=0}^{D} R_d \rho_d(u).$$

We define the d-dimensional *resel count* as

$$R_d = V_d / w_1^d, \qquad d = 0, \ldots, D,$$

where V_d are d-dimensional size measurements of the search region; in 3-D, V_0 is the Euler characteristic of the search region, V_1 is twice the average caliper diameter, V_2 is half the surface area, and V_3 is the volume. For 2-D data, V_0 is the Euler characteristic as before, V_1 is half the perimeter, and V_2 is the area (see Worsley *et al.* (1996a) for a more precise definition, methods of calculation, and examples). Let $r = w_1/w_2$, then the Euler characteristic (EC) intensities $\rho_d(u)$ are

$$\begin{aligned}
\rho_0(u) &= \int_u^\infty \frac{x^{\frac{\nu-2}{2}} e^{-\frac{x}{2}}}{2^{\frac{\nu}{2}}\Gamma\left(\frac{\nu}{2}\right)} dx + \frac{u^{\frac{\nu}{2}} e^{-\frac{u}{2}}}{2^{\frac{\nu-2}{2}}\Gamma\left(\frac{\nu}{2}\right)} \sqrt{\frac{D}{4\pi u}} (-\log_e r) \\
\rho_1(u) &= \frac{(4\log_e 2)^{\frac{1}{2}}}{(2\pi)^{\frac{1}{2}}} \frac{u^{\frac{\nu-1}{2}} e^{-\frac{u}{2}}}{2^{\frac{\nu-2}{2}}\Gamma\left(\frac{\nu}{2}\right)} \left\{ \frac{1+r}{2} + \sqrt{\frac{D}{4\pi u}} (1-r)[u-(\nu-1)] \right\} \\
\rho_2(u) &= \frac{(4\log_e 2)}{(2\pi)} \frac{u^{\frac{\nu-2}{2}} e^{-\frac{u}{2}}}{2^{\frac{\nu-2}{2}}\Gamma\left(\frac{\nu}{2}\right)} \left\{ \frac{1+r^2}{2} [u^2 - (\nu-1)] \right. \\
&+ \left. \sqrt{\frac{D}{4\pi u}} \frac{1-r^2}{2} \left[u^2 - (2\nu-1)u + (\nu-1)(\nu-2) + \frac{2}{D}u \right] \right\} \\
\rho_3(u) &= \frac{(4\log_e 2)^{\frac{3}{2}}}{(2\pi)^{\frac{3}{2}}} \frac{u^{\frac{\nu-3}{2}} e^{-\frac{u}{2}}}{2^{\frac{\nu-2}{2}}\Gamma\left(\frac{\nu}{2}\right)} \left\{ \frac{1+r^3}{2} [u^2 - (2\nu-1)u + (\nu-1)(\nu-2)] \right. \\
&+ \left. \sqrt{\frac{D}{4\pi u}} \frac{1-r^3}{3} \left[u^3 - 3\nu u^2 + 3(\nu-1)^2 u - (\nu-1)(\nu-2)(\nu-3) + \frac{6}{D}[u^2 - (\nu-1)u] \right] \right\}
\end{aligned}$$

5 Methods

We shall apply these results to a simple fMRI experiment where a subject was given a simple visual stimulus, flashing red dots, presented through light-tight goggles (Ouyang *et al.*, 1994). The stimulus was switched off for 4 scans, then on for 4 scans, and repeated 5 times, giving 40 scans in all, The time interval between scans was 6 seconds, giving a stimulus period of $T = 48$ seconds. The data set then consists of a time series of 40 2-D images, each 128 $\times$ 128 pixels on a 1.72mm pixel grid. Image number 20 is shown on the left of Figure 1, which is an oblique slice through the visual cortex in the lower part of the image. Darker shading represents higher blood flow. The time series at two pixels, one in the visual cortex and one outside, are also shown. There appears to be strong correlation with the stimulus at the lower pixel in the visual cortex, but none at the upper pixel outside the visual cortex. Let $Y(\mathbf{s}, t)$ represent the blood flow at location $\mathbf{s}$ in $D = 2$ dimensions and time t.

The standard deviation of fMRI data is not constant across the image, so the first step was to standardise the data to unit standard deviation at each pixel. To do this, a simple sine wave with period $T = 48$ seconds

$$\hat{Y}(\mathbf{s}, t) = m(\mathbf{s}) + b_1(\mathbf{s}) \sin(2\pi t/T) + b_2(\mathbf{s}) \cos(2\pi t/T)$$

was fitted to the blood flow data with coefficients estimated by

$$\begin{aligned} m(\mathbf{s}) &= \sum_t Y(\mathbf{s}, t)/n, \\ b_1(\mathbf{s}) &= \sum_t \sin(2\pi t/T) Y(\mathbf{s}, t)/(n/2), \\ b_2(\mathbf{s}) &= \sum_t \cos(2\pi t/T) Y(\mathbf{s}, t)/(n/2), \end{aligned}$$

where summation is over $n = 40$ scans. The pixel standard deviation is then estimated by

$$\sigma(\mathbf{s}) = \left(\sum_t [Y(\mathbf{s}, t) - \hat{Y}(\mathbf{s}, t)]^2/(n-3) \right)^{\frac{1}{2}},$$

and the standardised data is

$$Y^*(\mathbf{s}, t) = [Y(\mathbf{s}, t) - m(\mathbf{s})]/\sigma(\mathbf{s}),$$

which should now have equal standard deviation across all pixels.

The sine and cosine coefficients were re-estimated using the standardised data, to give

$$\begin{aligned} b_1^*(\mathbf{s}) &= \sum_t \sin(2\pi t/T) Y^*(\mathbf{s}, t)/(n/2), \\ b_2^*(\mathbf{s}) &= \sum_t \cos(2\pi t/T) Y^*(\mathbf{s}, t)/(n/2). \end{aligned}$$

These were then smoothed using a Gaussian filter with FWHMs w =5.0, 6.0, 7.1, 8.5, 10.2, 12.2, 14.6, 17.5, 20.9, 25.0mm equally spaced on a log scale to give uniform coverage of scale space (see Worsley *et al.*, 1996b):

$$b_i^*(\mathbf{s}, w) = K^*(w) \sum_{\mathbf{h}} f[(\mathbf{h} - \mathbf{s})/w] b_i^*(\mathbf{h}), \quad i = 1, 2,$$

where, because we have replaced an integral by a summation,

$$K^*(w) = \left(\sum_{\mathbf{h}} f[\mathbf{h}/w]^2 \right)^{-\frac{1}{2}}.$$

Note that although $b_i^*(\mathbf{s})$ is not exactly Gaussian, since it was divided by an estimated (random) standard deviation, the central limit theorem should ensure that $b_i^*(\mathbf{s}, w)$ is closer to Gaussian, if w is reasonably large, since it is a (weighted) sum of $b_i^*(\mathbf{s})$.

However the above method of constructing Gaussian scale space images may not ensure that $b_i^*(\mathbf{s}, w)$ has unit standard deviation. This is because, although $b_i^*(\mathbf{s})$ usually has very low spatial correlation for fMRI data, it is not quite zero and so $b_i^*(\mathbf{s})$ is not exactly white noise. Positive correlation, for example, will increase the standard deviation of $b_i^*(\mathbf{s}, w)$, and this was in fact observed. Since $b_i^*(\mathbf{s})$ and hence $b_i^*(\mathbf{s}, w)$ should have constant standard deviation across the image, this suggests that a global correction for the standard deviation is all that is necessary. To do this, the global standard deviation of the smoothed data was estimated separately using the coefficients at two periodicities, $A = 240/6$ and $B = 240/4$ seconds, either side of the periodicity of the signal ($T = 240/5$ seconds), that is

$$\begin{aligned}
a_1^*(\mathbf{s}) &= \sum_t \sin(2\pi t/A) Y^*(\mathbf{s}, t)/(n/2), \\
a_2^*(\mathbf{s}) &= \sum_t \cos(2\pi t/A) Y^*(\mathbf{s}, t)/(n/2). \\
c_1^*(\mathbf{s}) &= \sum_t \sin(2\pi t/C) Y^*(\mathbf{s}, t)/(n/2), \\
c_2^*(\mathbf{s}) &= \sum_t \cos(2\pi t/C) Y^*(\mathbf{s}, t)/(n/2).
\end{aligned}$$

These were smoothed as above:

$$\begin{aligned}
a_i^*(\mathbf{s}, w) &= K^*(w) \sum_{\mathbf{h}} f[(\mathbf{h} - \mathbf{s})/w] a_i^*(\mathbf{h}), \\
c_i^*(\mathbf{s}, w) &= K^*(w) \sum_{\mathbf{h}} f[(\mathbf{h} - \mathbf{s})/w] c_i^*(\mathbf{h}), \quad i = 1, 2.
\end{aligned}$$

These four images should contain no signal, and if the global variance (averaged over all pixels) is smooth in the frequency, then the average of these global variances, which linearly interpolates the variance across frequency, should be a good estimator of the global variance of $b_i^*(\mathbf{s}, w)$. Thus the estimator of the global variance is

$$\sigma^2(w) = \sum_{\mathbf{s}} [a_1^*(\mathbf{s}, w)^2 + a_2^*(\mathbf{s}, w)^2 + c_1^*(\mathbf{s}, w)^2 + c_2^*(\mathbf{s}, w)^2]/(4N),$$

where N is the number of pixels in the image. This was validated by repeating the operations for the upper part of the image, outside the visual cortex, where no signal should be present, and there was good agreement between $\sigma^2(w)$ and the mean sum of squares of $b_i^*(\mathbf{s}, w)$. Our final definition of the scale space Gaussian images is therefore

$$Z_i(\mathbf{s}, w) = b_i^*(\mathbf{s}, w)/\sigma(w), \quad i = 1, 2,$$

and the χ^2 field with $\nu = 2$ degrees of freedom is

$$U(\mathbf{s}, w) = Z_1(\mathbf{s}, w)^2 + Z_2(\mathbf{s}, w)^2.$$

The same considerations as mentioned above also affect the smoothness of the scale space data. The P-value formula in fact depends on the effective FWHM of the image, defined as

$$w_{\text{eff}} = \sqrt{\frac{4 \log_e 2}{|\mathbf{\Lambda}|^{\frac{1}{D}}}}, \qquad \mathbf{\Lambda} = \text{Var}\left(\frac{\partial Z_i(\mathbf{s}, w)}{\partial s}\right).$$

This was estimated from the pure noise images $a_i^*(\mathbf{s}, w)$ and $c_i^*(\mathbf{s}, w)$ by replacing derivatives by differences at adjacent pixels (Worsley *et al.*, 1992), then pooling the variance over all pixels and images. The results were w_{eff} =6.2, 7.5, 9.2, 11.3, 13.9, 17.1, 20.7, 24.7, 29.3, 34.4mm respectively, approximately 35% higher than the nominal FWHMs. Thus $w_1 =$ 6.2mm and $w_2 = 34.4$mm were used in the P-value formula in place of the nominal values of 5mm and 25mm, respectively.

6 Results

Figure 2, panels 1 and 2, show images of the sine and cosine coefficients $b_1(\mathbf{s})$ and $b_2(\mathbf{s})$. Some activation is clearly present in the cosine image in the lower portion of the image, corresponding to the visual cortex, as expected. To check sensitivity, three simulated Gaussian-shaped signals were created with lags of 0, 6 and 12 seconds, and widths of 9mm, 15mm and 25mm, respectively. Since no signal was expected outside the visual cortex (and none was in fact detected), these three signals were located in the upper half of the image (Figure 2, panels 3 and 4) and added to $b_1(\mathbf{s})$ and $b_2(\mathbf{s})$. The resulting magnitude of the periodogram $b_1(\mathbf{s})$ and $b_2(\mathbf{s})$ is shown , without the signal in Figure 2, panel 5, and with the signal added in panel 6. The remaining panels 10 panels in Figure 2 show slices of the scale space χ^2 fields $U(\mathbf{s}, w)$.

For the purpose of finding the P-value, the search region was approximated by a circle of radius $v = 61.7$mm chosen so that its area matched that of the set of pixels shown in Figures 1 and 2. This gives $V_0 = 1$, $V_1 =$ perimeter$/2 = \pi v = 194$mm and $V_2 =$ area $= \pi v^2 = 11960\text{mm}^2$. The P-value was then calculated as above with $D = 2$, $w_1 = 6.2$mm and $r = 6.2/34.4 = 0.18$. To find the $P = 0.05$ threshold, this was equated to 0.05 and solved for u to give $u = 25.3$. Scale space local maxima above this threshold are marked by white crosses on Figure 2. All three simulated signals are detected at w_{eff} =7.5, 13.9, 24.7mm FWHM, close to their actual widths of 9, 15, 25mm FWHM, respectively (panels 8, 11 and 14). Several local maxima appear in the visual cortex, culminating in the global maximum of $U_{\max} = 208$ in panel 15 at 29.3mm FWHM smoothing.

The scale space set of supra-threshold voxels at the $u = 25.3$ threshold is shown in Figure 3a. Four components are clearly evident: the three simulated signals in the upper part of the figure and the activation in the visual cortex in the lower part. The supra-threshold set at a much higher threshold $u = 175$ is shown in Figure 3b, this time tilted to emphasize the scale dimension. Four connected components are clearly visible corresponding to the three simulated signals and the activation in the visual cortex. Note that each of the simulated

signals is optimally detected at a filter width close to the width of the signal, as predicted by the Matched Filter Theorem. The stimulus is detected at all scales, suggesting a mix of sharp foci of activation embedded in a broader 'penumbra' of lesser activation. This is more clearly seen at 11.3mm smoothing (Figure 2, panel 10). The sharp foci may correspond to arterial blood flow, whereas the penumbra may correspond to blood flow in the capillaries.

References

Bullmore, E.T., Brammer, M.J., Williams, S.C.R., Rabe-Hesketh, S., Janot, N., David, A.S., Mellers, J.D.C., Howard, R. & Sham, P. (1996). Statistical methods of estimation and inference for functional MR image analysis. *Magnetic Resonance in Medicine*, 35:261-277.

Friston, K.J., Jezzard, P. & Turner, R. (1994a). Analysis of functional MRI time series. *Human Brain Mapping*, 1:153-171.

Friston, K.J., Worsley, K.J., Frackowiak, R.S.J., Mazziotta, J.C. & Evans, A.C. (1994b). Assessing the significance of focal activations using their spatial extent. *Human Brain Mapping*, 1:214-220.

Friston, K.J., Holmes, A.P., Poline, J-B., Grasby, B.J., Williams, C.R., Frackowiak, R.S.J., & Turner, R. (1995). Analysis of fMRI time-series revisited. *NeuroImage*, 2:45-53.

Lange, N. & Zeger, S.L. (1996). Non-linear Fourier time series analysis for human brain mapping by functional magnetic resonance imaging. *Applied Statistics*, in press.

Ouyang, X., Pike, G.B. & Evans, A.C. (1994). fMRI of human visual cortex using temporal correlation and spatial coherence analysis. *13th Annual Symposium of the Society of Magnetic Resonance in Medicine*.

Poline J.B. & Mazoyer B.M. (1994). Enhanced detection in brain activation maps using a multifiltering approach. *Journal of Cerebral Blood Flow and Metabolism*, 14:639-42.

Rosenfeld, A. & Kak, A.C. (1982). *Digital Picture Processing, Volume 2.* Academic Press, Orlando.

Siegmund, D.O & Worsley, K.J. (1995). Testing for a signal with unknown location and scale in a stationary Gaussian random field. *Annals of Statistics*, 23:608-639.

Worsley, K.J. (1997). Testing for a signal with unknown location and scale in a χ^2 random field, with an application to fMRI. *Annals of Statistics*, submitted.

Worsley, K.J., Evans, A.C., Marrett, S. & Neelin, P. (1992). A three dimensional statistical analysis for CBF activation studies in human brain. *Journal of Cerebral Blood Flow and Metabolism*, 12:900-918.

Worsley, K.J., & Friston, K.J. (1995). Analysis of fMRI time-series revisited - again. *NeuroImage*, 2:173-181.

Worsley, K.J., Marrett, S., Neelin, P., Vandal, A.C., Friston, K.J., & Evans, A.C. (1996a). A unified statistical approach for determining significant signals in images of cerebral activation. *Human Brain Mapping*, 4:58-73.

Worsley, K.J., Marrett, S., Neelin, P., & Evans, A.C. (1996b). Searching scale space for activation in PET images. *Human Brain Mapping*, 4:74-90.

Figure 1. Blood flow (jagged lines) at two pixels chosen to illustrate
correlation (lower) and no correlation (upper) with the stimulus (dashed line)

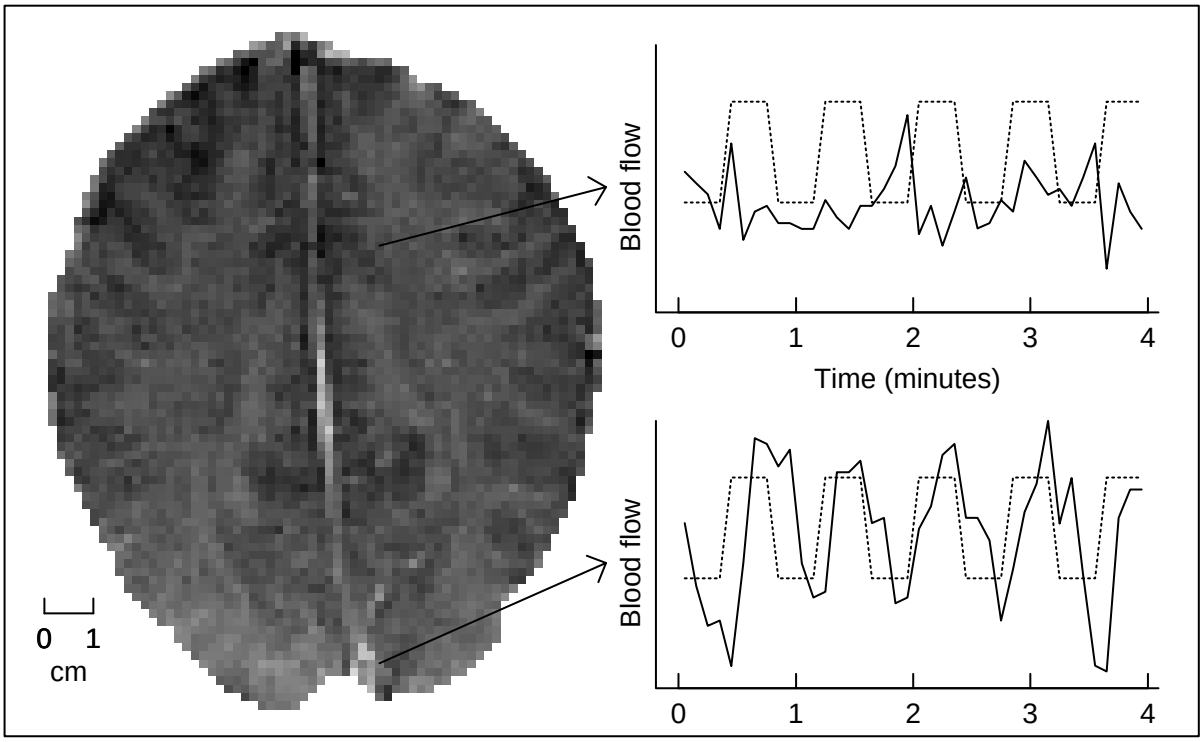

Figure 1: One of 40 fMRI images of the human brain while the subject was responding to an on-off visual stimulus repeated five times. The image shows an oblique slice through the visual cortex in the lower part of the image. Darker shading represents higher cerebral blood flow. The time series (jagged lines) at two pixels, one in the visual cortex and one outside, are also shown. There appears to be strong correlation with the stimulus (dashed lines) at the lower pixel in the visual cortex, but none at the upper pixel outside the visual cortex.

Figure 2. Scale space analysis of data + simulated signal

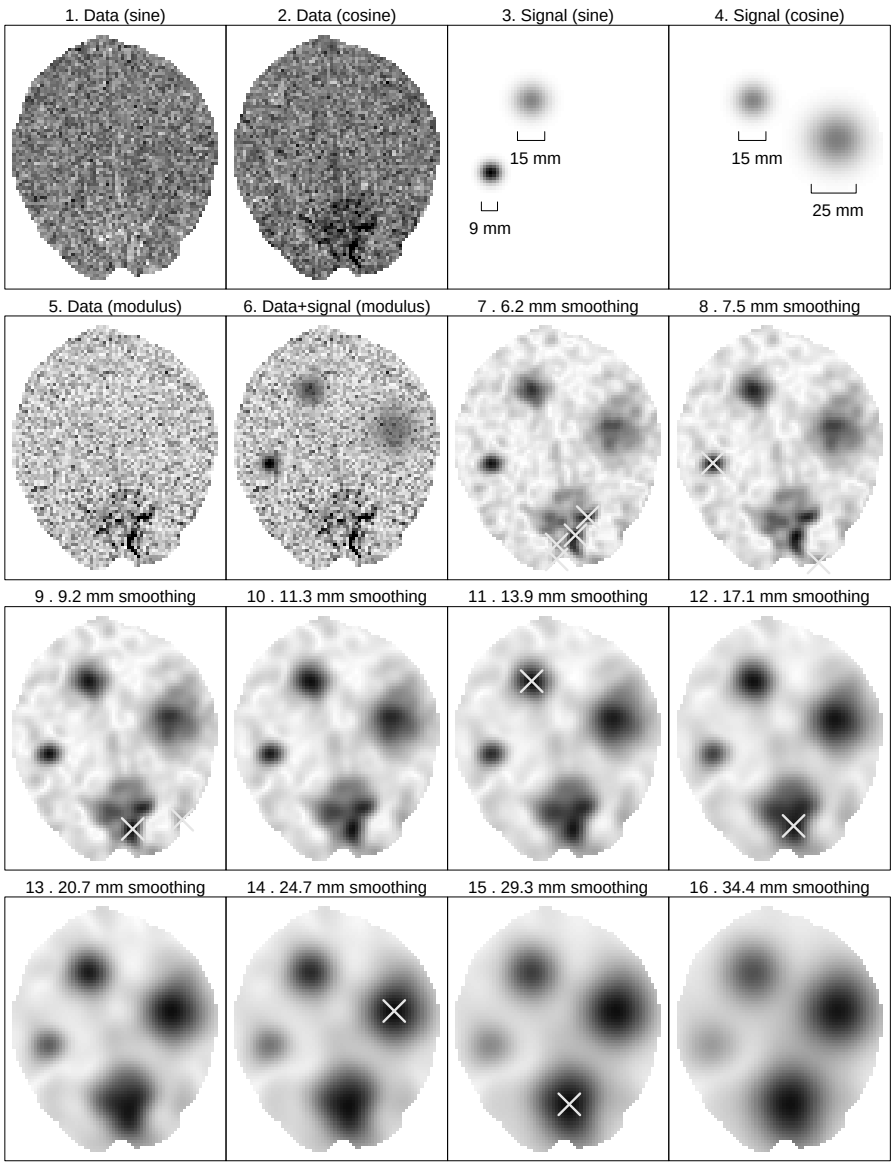

Figure 2: Unsmoothed cross-covariance of the 40 images with sine and cosine functions whose frequency matches that of the stimulus to give $b_1^*(\mathbf{s})$ (panel 1) and $b_2^*(\mathbf{s})$ (panel 2), respectively. Three simulated Gaussian-shaped signals with lags of 0, 6 and 12 seconds, and 9mm, 15mm and 25mm FWHM, respectively, were added to the sine (panel 3) and cosine (panel 4) components. Panel 5 shows the sum of squares of the sine and cosine components, $U(\mathbf{s})$. Panels 6–15 show the sum of squares of the sine and cosine components $U(\mathbf{s}, w)$, separately smoothed by a Gaussian-shaped kernel varying from 6.2mm to 34.4mm effective FWHM. Scale space local maxima above the approximate $P = 0.05$ critical threshold for $U_{\max}$ ($u = 25.3$) are marked by a white cross. All three simulated signals are detected at w_{eff} =7.5, 13.9, 24.7mm FWHM, close to their actual widths of 9, 15, 25mm FWHM, respectively (panels 8, 11 and 14). Several local maxima appear in the visual cortex, culminating in the global maximum of $U_{\max} = 208$ in panel 15 at 29.3mm FWHM smoothing.

Figure 3a. Scale space supra-threshold
voxels above u=25.3 (P=0.05)

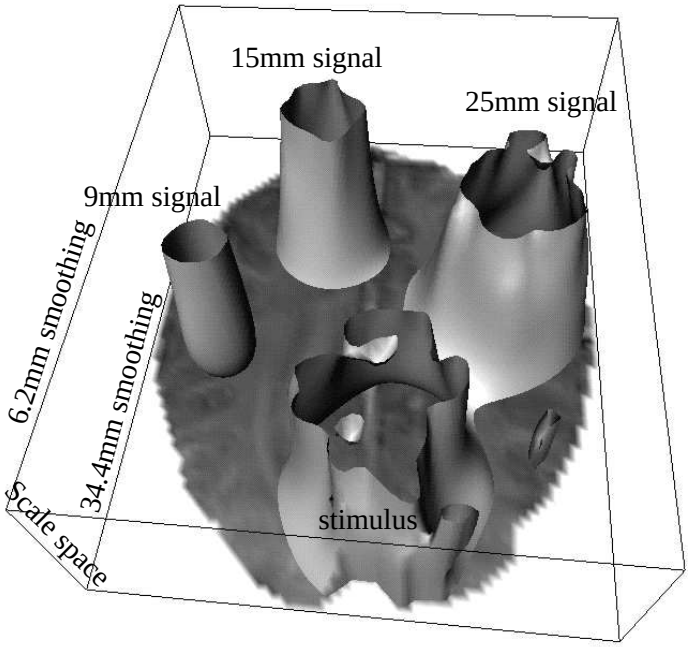

Figure 3b. Scale space supra-threshold voxels above u=175

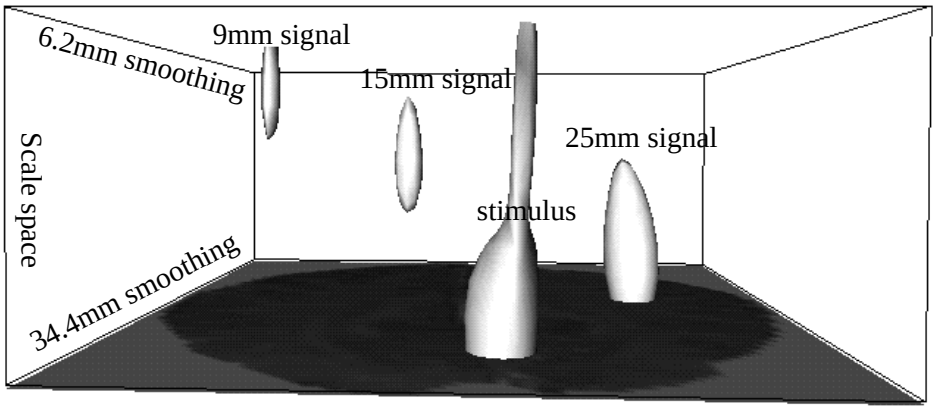

Figure 3: The scale space set of supra-threshold voxels above (a) $u = 25.3$, the approximate $P = 0.05$ critical threshold for $U_{\max}$, and (b) a higher threshold $u = 175$. Four components are clearly evident: the three simulated signals in the upper part of the figure and the activation in the visual cortex in the lower part. Note in (b) that each of the simulated signals is optimally detected at a filter width close to the width of the signal, as predicted by the Matched Filter Theorem. The stimulus is detected at all scales, suggesting a mix of sharp foci of activation embedded in a broader 'penumbra' of lesser activation, visible in Figure 2, panel 10.